J Mater Sci: Mater Electron
DOI 10.1007/s10854-017-7275-x

Microwave dielectric properties of temperature-stable $(Mg_{0.95}Co_{0.05})_2TiO_4$–$Li_2TiO_3$ composite ceramics for LTCC applications

Haiyu Wang[1] · Hua Su[1,2] · Yuanming Lai[1] · Huaiwu Zhang[1] · Yuanxun Li[1,2] · Xiaoli Tang[1]

Received: 10 May 2017 / Accepted: 1 June 2017

Abstract In this paper, the effects of Li_2O–B_2O_3–Bi_2O_3–SiO_2 (LBBS) glass on the phase formation, sintering characteristic, the microstructure and microwave dielectric properties of temperature-stable $(Mg_{0.95}Co_{0.05})_2TiO_4$–$Li_2TiO_3$ ceramics were investigated. $(Mg_{0.95}Co_{0.05})_2TiO_4$–$Li_2TiO_3$ powders were obtained by using the traditional solid-state process. A small amount of LBBS doping can effectively reduce sintering temperature and promote the densification of the ceramics. X-ray diffraction analysis revealed not only the primary phase $(Mg{\cdot}Co)_2TiO_4$ associated with Li_2TiO_3 minor phase but also a third phase $(Mg{\cdot}Co)TiO_3$. The dielectric constant and *Qf* values vary with the doping amount of LBBS and sintering temperatures. With the compensation of the positive temperature coefficient (τ_f) of Li_2TiO_3 and the negative τ_f of $(Mg_{0.95}Co_{0.05})_2TiO_4$, the τ_f of the specimens fluctuates around zero. The $(Mg_{0.95}Co_{0.05})_2TiO_4$ ceramic with 2.5 wt% LBBS addition and sintering at 900 °C for 4 h exhibited excellent microwave dielectric properties: $\varepsilon_r = 19.076$, $Qf = 126100$ GHz, and $\tau_f = 0.98$ ppm/°C.

1 Introduction

With the rapid development of microwave communication, the demand for microwave ceramic components has intensified. To realize the miniaturization and integration of microwave devices, low temperature co-fired ceramic (LTCC) technology has been studied extensively. Given its high conductivity and low cost, silver (Ag) has been widely used as internal electrodes in LTCC devices [1–5]. The melting point of silver is in the vicinity of 960 °C. Thus, the sintering temperature of LTCC materials must be lower than 960 °C [6–8]. In recent years, three main methods have been used to reduce the sintering temperature of these dielectric ceramics; these methods are low melting glass addition, chemical processing, and small particle size of starting materials [9–12]. A small τ_f of LTCC materials is also important to obtain stable LTCC microwave components [13–16]. Mg_2TiO_4 ceramics are frequently used dielectric ceramics because of their excellent microwave dielectric properties, namely, ε_r value of ~14, a high *Qf* value of ~150,000, and τ_f of ~−50 ppm/°C when sintered at 1350 °C. Mg^{2+} ions can be substituted by Co^{2+} ions to form $(Mg{\cdot}Co)_2TiO_4$ compositions. $(Mg_{0.95}Co_{0.05})_2TiO_4$ ceramics with a spinel-type structure have excellent dielectric properties with a ε_r value ~15.7, a *Qf* value of ~286,000 GHz and a τ_f value of ~−52.5 ppm/°C [17–19]. However, the τ_f value of $(Mg_{0.95}Co_{0.05})_2TiO_4$ ceramics is significantly negative. Thus, the practicality of this material is limited. Li_2TiO_3 not only has a relatively low sintering temperature but also has a positive τ_f ($\varepsilon_r = 12$, $Qf = 15{,}000$, $\tau_f = 35.05$ ppm/°C) [20]. To achieve a near-zero τ_f value, the $(Mg_{0.95}Co_{0.05})_2TiO_4$ and Li_2TiO_3 are compounded at proper contents. However, the sintering temperature of $(Mg_{0.95}Co_{0.05})_2TiO_4$–$Li_2TiO_3$ is still higher than 950 °C. Thus, an appropriate sintering aid must be used to reduce the sintering temperature of $(Mg_{0.95}Co_{0.05})_2TiO_4$–$Li_2TiO_3$.

In this work, Li_2O–B_2O_3–Bi_2O_3–SiO_2 (LBBS) glass was used as a sintering aid to lower the sintering temperature of $(Mg_{0.95}Co_{0.05})_2TiO_4$–$Li_2TiO_3$ compound ceramics. The

✉ Hua Su
uestcsh@163.com

[1] State Key Laboratory of Electronic Thin Films and Integrated Devices, University of Electronic Science and Technology of China, Chengdu 610054, China

[2] Institute of Electronic and Information Engineering, University of Electronic Science and Technology of China, Dongguan 518105, China

Published online: 06 June 2017

effects of this glass on the sintering behavior, microstructure, and microwave dielectric properties of the ceramics were systematically investigated.

2 Experimental procedure

High-purity MgO (99.5%), Co_2O_3 (99.5%), Li_2CO_3 (99.5%) and TiO_2 (99.5%), were used as starting materials. The powders were prepared separately according to the desired stoichiometry Li_2TiO_3 and $(Mg_{0.95}Co_{0.05})_2TiO_4$ and then milled with ZrO_2 balls in distilled water for 12 h. The prepared $(Mg_{0.95}Co_{0.05})_2TiO_4$ powders were dried and calcined at 1150 °C for 4 h in air. The prepared Li_2TiO_3 powders were dried and calcined at 850 °C for 4 h in air. LBBS glass was prepared using a quenching method. The oxide raw materials were mixed and melted at 1150 °C for 2 h using an alumina crucible at a Li_2CO_3:B_2O_3:BiO_3:SiO_2 molar ratio of 2:2:1:1. The solution was then quickly removed from the furnace and poured with cold water to obtain the glass. Then, 0.5–3.5 wt% LBBS was added to $0.44(Mg_{0.95}Co_{0.05})_2TiO_4$–$0.56Li_2TiO_3$ (0.44:0.56 was the weight ratio of the $(Mg_{0.95}Co_{0.05})_2TiO_4$ and Li_2TiO_3 powders, which was calculated by their respective τ_f to obtain near-zero τ_f in the compound materials), ground in distilled water for 12 h in a ball mill with ZrO_2 balls, dried and mixed with 20 wt% acryloid as binder, and then granulated. The granulated powders were uniaxially pressed into pellets, which were sintered at 850–950 °C for 4 h.

The crystalline phases of the sintered ceramics were analyzed by using X-ray diffraction (XRD: DX-2700) using Cu K_α radiation, and microstructure observations were performed by using scanning electron microscopy (SEM: JOEL JSM6490LV). The relative densities were obtained by the ratios of the bulk and theoretical densities. The microwave dielectric characteristics of the sintered samples were measured using the Hakki–Coleman method with Agilent N5230A network analyzer in a resonant cavity. The temperature coefficient of resonant frequency (τ_f) can be calculated by the following equation: $\tau_f = (f_{80} - f_{20})/[f_{20} \times (80 - 20)]$, where f_{80} and f_{20} represent the resonant frequency at 80 and 20 °C, respectively [21–23].

3 Results and discussion

Figure 1 shows the XRD patterns of $0.44(Mg_{0.95}CO_{0.05})_2TiO_4$–$0.56Li_2TiO_3$ ceramics with x wt% LBBS ($x = 0.5$, 1, 1.5, 2, 2.5, 3, 3.5) and sintered at 900 °C. The XRD patterns shows that all samples have three phases, namely, the primary phase $(Mg{\cdot}Co)_2TiO_4$ associated with Li_2TiO_3 and the third phase $(Mg_vCo)TiO_3$. The formation of the second phase is attributed to the decomposition of

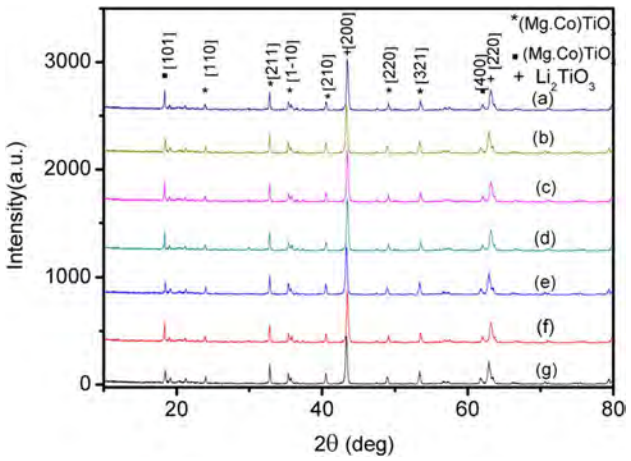

Fig. 1 XRD patterns of $(Mg_{0.95}Co_{0.05})_2TiO_4$–$Li_2TiO_3$ with x wt% LBBS: **a** $x = 0.5$, **b** $x = 1$, **c** $x = 1.5$, **d** $x = 2$, **e** $x = 2.5$, **f** $x = 3$, **g** $x = 3.5$

$(Mg_{0.95}Co_{0.05})_2TiO_4$ into $(Mg{\cdot}Co)_2TiO_4$ and $(Mg{\cdot}Co)TiO_3$, which was confirmed in a previous report [17]. LBBS addition was not found in the XRD patterns, thereby suggesting that LBBS existed in an amorphous phase [24].

Figure 2 shows the SEM micrographs of $0.44(Mg_{0.95}Co_{0.05})_2TiO_4$–$0.56Li_2TiO_3$ ceramics sintered at 900 °C for 3 h in air; these ceramics were added with different amounts of LBBS glass. LBBS have a strong effect on the average grain size and compactness of the compound ceramics. The sample with 0.5 wt% LBBS glass has a porous microstructure with a small average grain size. With the increase in the glass content, the average grain size enlarged obviously, and intergranular pores reduced significantly. This phenomenon is due to the low melting point of LBBS glass, which formed a liquid-phase layer and facilitated the liquid-phase sintering process. When the LBBS content reached 2.5 wt%, the microstructure became denser, and few intergranular pores were found. However, after incorporating large contents of LBBS glass at more than 3.5 wt%, the SEM micrographs showed a molten microstructure without a clear grain.

The effect of LBBS content on the apparent densities is shown in Fig. 3. The relative density of the samples increased slightly with the increase in the LBBS content, peaked with 2.5 wt% LBBS, and then decreased with a further increase in LBBS content. This phenomenon was also consistent with the change in microstructure. With the increase in the amount of LBBS glass, the densification of the samples increased and the number of intergranular pores reduced until the densification peaked with 2.5 wt% LBBS. The densification and the number of intergranular pores decreased with a further increase in LBBS content.

Figure 4 shows the ε_r values of $0.44(Mg_{0.95}Co_{0.05})_2TiO_4$–$0.56Li_2TiO_3$ samples with different doping amounts of LBBS and sintered at various temperatures. As expected,

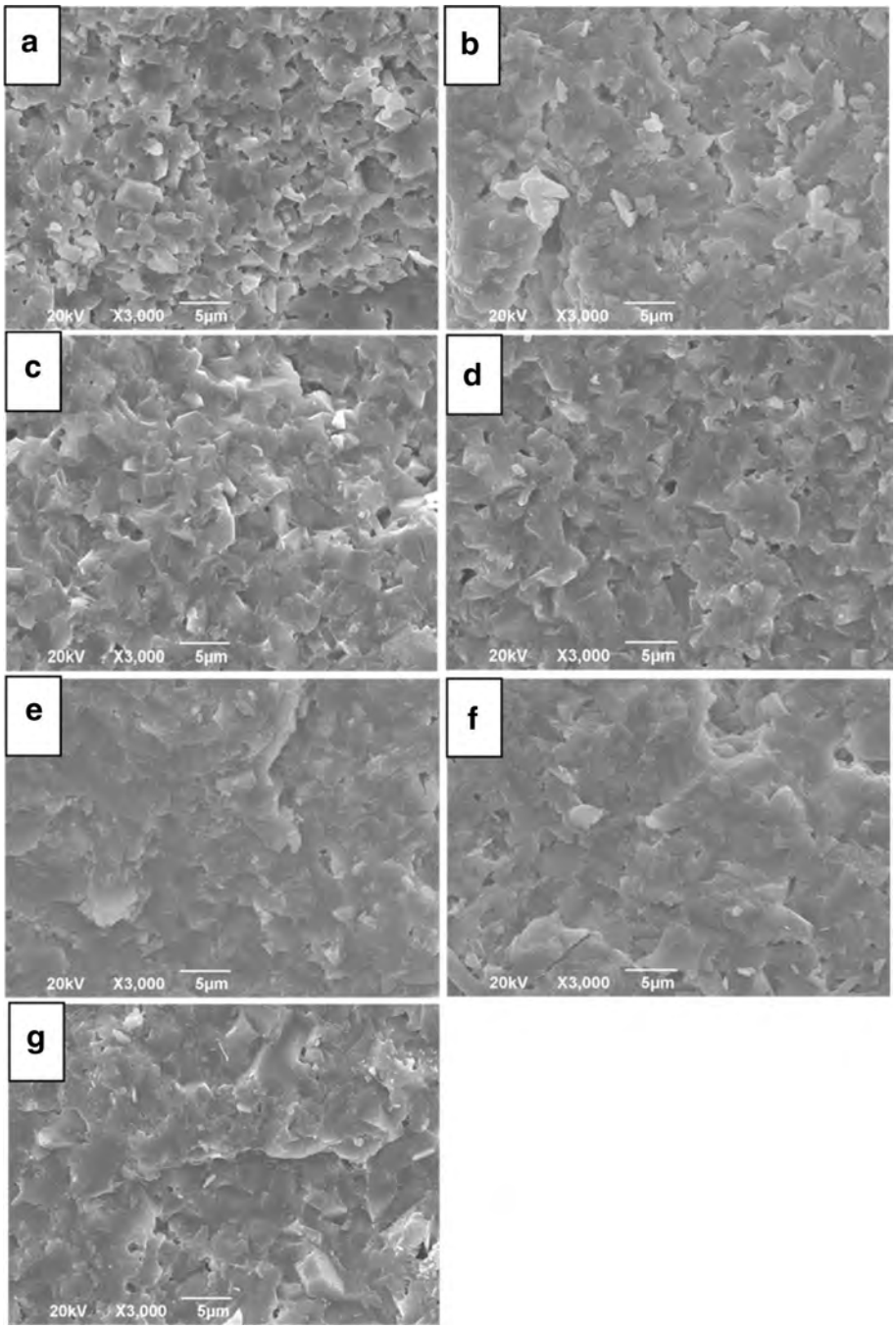

Fig. 2 SEM micrographs of $(Mg_{0.95}Co_{0.05})_2TiO_4$–$Li_2TiO_3$ with x wt% LBBS: **a** $x=0.5$, **b** $x=1$, **c** $x=1.5$, **d** $x=2$, **e** $x=2.5$, **f** $x=3$, **g** $x=3.5$

the tendency of ε_r values is consistent with the tendency of relative density. With the addition of LBBS glass, ε_r values increased gradually until they peaked with 2.5 wt% LBBS. Then, ε_r slightly decreased with further LBBS addition. The same tendency of ε_r values and relative density shows that the permittivity was significantly affected by the relative density.

Figure 5 shows the Qf values of LBBS-doped 0.44($Mg_{0.95}Co_{0.05})_2TiO_4$–$0.56Li_2TiO_3$ ceramics that were sintered at a temperature range from 850 to 950 °C. The *Qf* values of the sample sintered at 900 and 950 °C initially increased and peaked with 2.5 wt% LBBS and then decreased with the increase in the LBBS content. The *Qf* value changed minimally when the sample was sintered at 850 °C. Microwave dielectric loss may be divided into intrinsic and extrinsic losses. Intrinsic losses are primarily dependent on the crystal structure and are mainly caused by lattice vibration modes. Extrinsic losses are related to many factors, such as second phases, oxygen vacancies, grain sizes, and densification or porosity [3, 13, 19]. Therefore, the initial increase in the *Qf* value may be due to increased densification and average grain

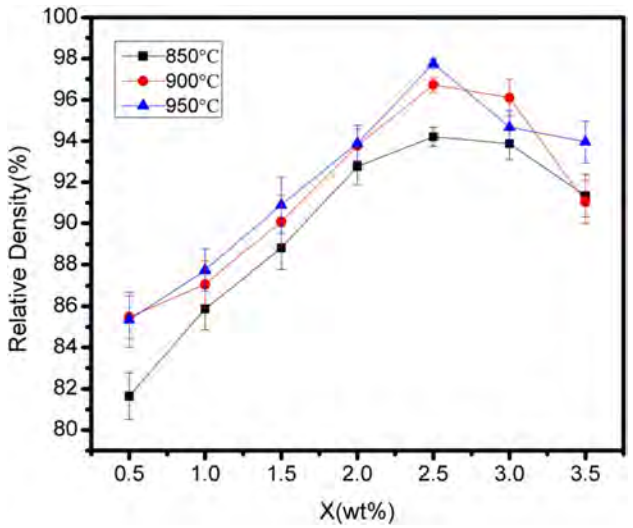

Fig. 3 Sintering densities values of $(Mg_{0.95}Co_{0.05})_2TiO_4$–$Li_2TiO_3$ with *x* wt% LBBS

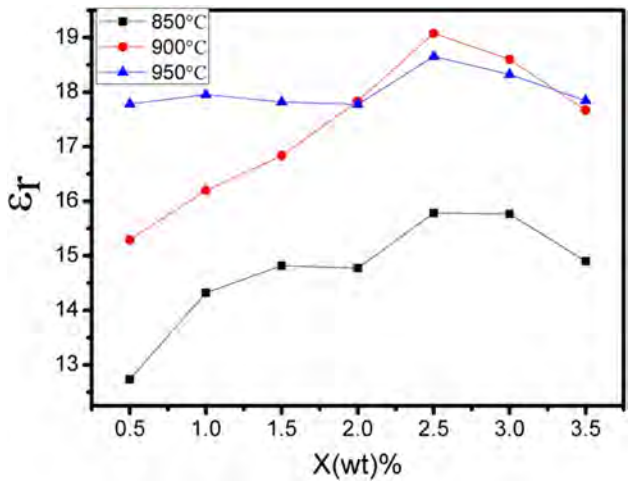

Fig. 4 ε_r of $(Mg_{0.95}Co_{0.05})_2TiO_4$–$Li_2TiO_3$with *x* wt% LBBS

size. The subsequent decrease in the *Qf* values may due to the increasing number of intergranular pores and the excessively high loss of the liquid glass phase.

Figure 6 shows the τ_f values of $0.44(Mg_{0.95}Co_{0.05})_2TiO_4$–$0.56Li_2TiO_3$ samples sintered at 900 °C for 4 h in air. τ_f can be tuned by the formation of a solid solution or mixtures of dielectrics with opposite τ_f values [13]. $(Mg_{0.95}Co_{0.05})_2TiO_4$ has τ_f values of −50 ppm/°C, and Li_2TiO_3 has τ_f values of 35.05 ppm/°C. Therefore, through recombination, Li_2TiO_3 with positive τ_f values and $(Mg_{0.95}Co_{0.05})_2TiO_4$ with negative τ_f values can obtain a composite with near-zero τ_f values.

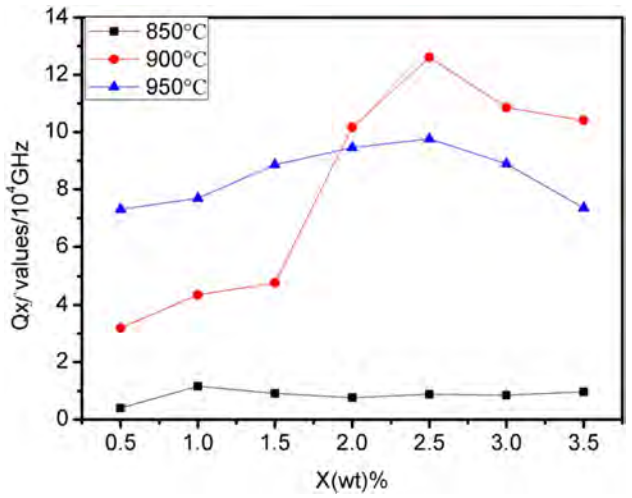

Fig. 5 *Qf* values of $(Mg_{0.95}Co_{0.05})_2TiO_4$–$Li_2TiO_3$ with different values of LBBS glass

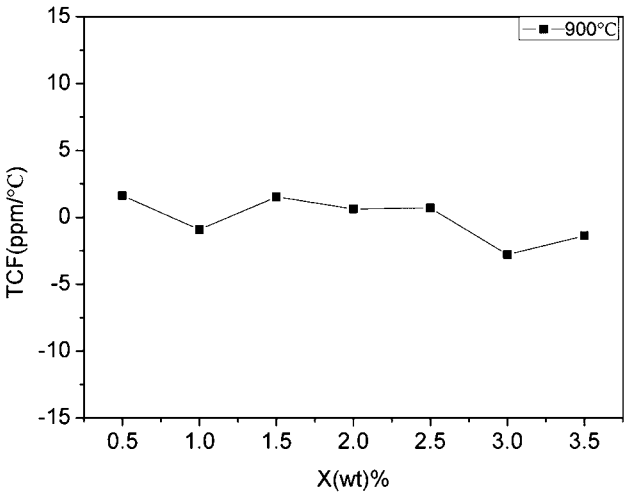

Fig. 6 τ_f values of $(Mg_{0.95}Co_{0.05})_2TiO_4$–$Li_2TiO_3$ with different amounts of LBBS

4 Conclusion

In this work, the effect of LBBS glass doping on sintering temperature, microstructure, and microwave dielectric properties of $0.44(Mg_{0.95}Co_{0.05})_2TiO_4$–$0.56Li_2TiO_3$ ceramics were investigated. Combining Li_2TiO_3 with positive τ_f and $(Mg_{0.95}Co_{0.05})_2TiO_4$ with negative τ_f could obtain $0.44(Mg_{0.95}Co_{0.05})_2TiO_4$–$0.56Li_2TiO_3$ samples with near-zero τ_f values. With moderate LBBS addition, high *Qf* values could be obtained. When the amount of LBBS doping was 2.5% and with sintering at 900 °C, the $0.44(Mg_{0.95}Co_{0.05})_2TiO_4$–$0.56Li_2TiO_3$ ceramics presented excellent microwave dielectric properties: $\varepsilon_r = 19.076$, $Qf = 126{,}100$ GHz and $\tau_f = 0.98$ ppm/°C, which is suitable for LTCC applications.

Acknowledgements This work was supported by the National Natural Science Foundation of China under Grant Nos. 61471096 and 51372031, Special Support Program of Guangdong Province under Grant No. 2014TX01C042 and Science and Technology Department of Sichuan Province 2016GZ0258, 2016JQ0016.

References

1. M.T. Sebastian, H. Jantunen, Int. Mater. Rev. **53**, 57 (2008)
2. C.S. Hsi, Y.R. Chen, H.I. Hsiang, J. Mater. Sci **46**, 4695 (2011)
3. M. Guo, S. Gong, G. Dou, D. Zhou, J. Alloys Compd. **509**, 5988 (2011)
4. Z.B.O. Frit **954**, 2008 (2009)
5. G. hua Chen, L. jiang Tang, J. Cheng, M. hong Jiang, J. Alloys Compd. **478**, 858 (2009)
6. A. Feteira, D.C. Sinclair, J. Am. Ceram. Soc. **91**, 1338 (2008)
7. G. Yao, P. Liu, H. Zhang, J. Am. Ceram. Soc. **96**, 1691 (2013)
8. H. Chen, H. Su, H. Zhang, T. Zhou, B. Zhang, J. Zhang, X. Tang, Ceram. Int. **1088**, 1 (2014)
9. Z. Zhang, H. Su, X. Tang, H. Zhang, T. Zhou, and Y. Jing, Ceram. Int. **40**, 1613 (2014)
10. C.-L. Huang, J.-Y. Chen, J. Am. Ceram. Soc. **92**, 379 (2009)
11. N.X. Wu, J.J. Bian, Int. J. Appl. Ceram. Technol. **8**, 1494 (2011)
12. J. Tong, B. Zhang, W. Huang, H. Yang, Mater. Lett. **95**, 168 (2013)
13. S. Zhang, H. Su, H. Zhang, Y. Jing, X. Tang, Ceram. Int. **42**, 15242 (2016)
14. C.F. Tseng, P.H. Chen, P.A. Lin, J. Alloys Compd. **632**, 810 (2015)
15. G. Yao, P. Liu, H. Zhang, J. Am. Ceram. Soc. **96**, 3119, (2013)
16. W. Lei, W.Z. Lu, X.C. Wang, Ceram. Int. **38**, 99 (2012)
17. C.-L. Huang, J.-Y. Chen, B.-J. Li, Mater. Chem. Phys. **120**, 217 (2010)
18. C.L. Huang, J.Y. Chen, J. Alloys Compd. **485**, 706 (2009)
19. M. Guo, G. Dou, S. Gong, D. Zhou, J. Eur. Ceram. Soc. **32**, 883 (2012)
20. A. Sayyadi-Shahraki, E. Taheri-Nassaj, S.A. Hassanzadeh-Tabrizi, H. Barzegar-Bafrooei, J. Alloys Compd. **597**, 161 (2014)
21. J.S. Chen, G.H. Chen, X.L. Kang, T. Yang, Z.C. Li, Y. Yang, C.L. Yuan, C.R. Zhou, J. Mater. Sci. Mater. Electron. **28**, 317 (2017)
22. H. Zhou, N. Wang, X. Tan, J. Huang, X. Chen, J. Mater. Sci. Mater. Electron. **27**, 11850 (2016)
23. F. Gu, G. Chen, C. Yuan, C. Zhou, T. Yang, Y. Yang, Mater. Res. Bull. **61**, 245 (2015)
24. R.-L. Jia, H. Su, X.-L. Tang, Y.-L. Jing, Chinese Phys. B **23**, 47801 (2014)